NMR MEASUREMENT OF OIL SHALE MAGNETIC RELAXATION AT HIGH MAGNETIC FIELD

Joseph D. Seymour[1,2], Kathryn E. Washburn[3], Catherine M. Kirkland[1,2], Sarah J. Vogt[1,2,4], Justin E. Birdwell[5] and Sarah L. Codd[2,6]

[1] Department of Chemical and Biological Engineering, Montana State University, Bozeman, MT

[2] Center for Biofilm Engineering, Montana State University, Bozeman, MT

[3] Weatherford Laboratories, 8845 Fallbrook Drive, Houston, TX

[4] School of Mechanical and Chemical Engineering, University of Western Australia, Crawley, WA, Australia

[5] U.S. Geological Survey, Denver Federal Center, Denver, CO

[6] Department of Mechanical and Industrial Engineering, Montana State University, Bozeman, MT

This paper was prepared for presentation at the International Symposium of the Society of Core Analysts held in Napa Valley, California,, USA, 16-19 September, 2013.

ABSTRACT

Nuclear magnetic resonance (NMR) at low field is used extensively to provide porosity and pore-size distributions in reservoir rocks. For unconventional resources, due to low porosity and permeability of the samples, much of the signal exists at very short T_2 relaxation times. In addition, the organic content of many shales will also produce signal at short relaxation times. Despite recent improvements in low-field technology, limitations still exist that make it difficult to account for all hydrogen-rich constituents in very tight rocks, such as shales. The short pulses and dead times along with stronger gradients available when using high-field NMR equipment provides a more complete measurement of hydrogen-bearing phases due to the ability to probe shorter T_2 relaxation times ($<10^{-5}$ sec) than can be examined using low-field equipment. Access to these shorter T_2 times allows for confirmation of partially resolved peaks observed in low-field NMR data that have been attributed to solid organic phases in oil shales. High-field (300 MHz or 7 T) NMR measurements of spin-spin T_2 and spin-lattice T_1 magnetic relaxation of raw and artificially matured oil shales have potential to provide data complementary to low field (2 MHz or 0.05T) measurements. Measurements of high-field T_2 and T_1-T_2 correlations are presented. These data can be interpreted in terms of organic matter phases and mineral-bound water known to be present in the shale samples, as confirmed by Fourier transform infrared spectroscopy, and show distributions of hydrogen-bearing phases present in the shales that are similar to those observed in low field measurements.

INTRODUCTION

High field nuclear magnetic resonance (NMR) has been used to study oil shales and kerogen. The primary approaches applied to characterization of shales has been solid state NMR of kerogen isolated from the dissolved mineral matrix using ^{13}C cross polarization, magic angle spinning and heteronuclear correlation techniques for chemical and structural analysis of the kerogen [1-3]. Other solid state NMR has used ^{1}H solid echo transverse relaxation during heating of powdered shales[4]. These studies provide no information on the kerogen distribution within and interaction with the mineral matrix pertinent to understanding the structure of shales. NMR

well logging has a long and well documented history in characterizing geologic formations [5] and NMR is a premier method for characterizing porous media based on the impact of the pore fluid molecular dynamics on magnetic relaxation[6]. Spin-spin transverse T_2 relaxation and spin-lattice longitudinal T_1 relaxation depend on the pore structure through the surface to volume ratio[7]. Multidimensional magnetic relaxation correlation experiments have been demonstrated to provide significant data for characterization of geological porous media with fluid saturated pore spaces [8] as well as protein gels where pore spaces are less well defined[9]. Recent advances in low field NMR technology have allowed measurement of NMR relaxation correlations in oil shales at 2 MHz [10]. This work explores the ability of high field NMR measurements of relaxation correlations to inform and extend characterization of the structure of shales. At a basic level oil shale is a solid mineral matrix filled with and containing regions of macromolecular networks of kerogen. Data on the distribution and thermophysical state of the kerogen is limited. Green River and Rundle kerogen has been shown to exhibit glassy state polymer behavior by ^{1}H solid state NMR with a transition to a rubbery state above the glass transition temperature[4]. Atomic force microscopy (AFM) has been used to probe kerogen in Woodford shale and indicates an isotropic rigid polymer of elastic and plastic deformation response[11]. NMR relaxation measurements may provide details on the physical state of the polymer and the distribution in the mineral matrix.

THEORY

Spin-lattice T_1 relaxation of the NMR signal occurs due to interaction in the longitudinal direction along the applied magnetic field B_0, and spin-spin dipolar T_2 relaxation occurs due to interactions transverse to B_0. The T_2 relaxation is dependent on rotational mobility of the proton ^{1}H nuclei. For protons on macromolecular polymers, T_2 is on the order of milliseconds while in bulk water it is on the order of seconds. The measurement of T_2 using a standard CPMG pulse sequence[12], is sensitive to the time scale of the measurement, in particular the 2τ time spacing between the 180 degree radio frequency (rf) pulses in terms of refocusing background gradient fields and hydrogen exchange which can occur in polymer solvent systems. In the case where background internal gradients can be ignored due to short echo time (180 rf pulse spacing) the relaxation rates for fluid imbibed in soil pore matrices

$$\frac{1}{T_i} = \frac{1}{T_{i\_bulk}} + \rho_i \frac{S}{V} \qquad (1)$$

depend on ρ_i is the surface relaxivity of the pore surface for T_i, S is the pore surface area, V the volume of the pores. and T_{i_bulk} is the bulk fluid relaxation time and i = 1 or 2 for spin-lattice or spin-spin relaxation[13]. The relaxation of fluid in porous media is influenced by pore size through the S/V ratio. Measurement of NMR signal attenuation and inversion to obtain the distribution of relaxation times provides a pore size distribution. In oil shales hydrogen is present in organic materials such as kerogen rather than as a pore fluid. NMR relaxation of semi-solids such as crosslinked polymers is dominated by intramolecular dipolar coupling[14]. Relaxation is dependent on the rotational correlation time τ_c of the molecular dynamics which generate the fluctuations in magnetic field through dipolar coupling as

$$\frac{1}{T_1} = \left(\frac{6}{20}\right) \times \left(\frac{\hbar^2 \gamma_I^2 \gamma_S^2}{r^6}\right) \times \left(\frac{\tau_c}{1+\omega_0^2\tau_c^2} + \frac{4\tau_c}{1+4\omega_0^2\tau_c^2}\right) \qquad (2)$$

for spin-lattice relaxation and

$$\frac{1}{T_2} = \left(\frac{3}{20}\right) \times \left(\frac{\hbar^2 \gamma_I^2 \gamma_S^2}{r^6}\right) \times \left(3\tau_c + \frac{5\tau_c}{1+\omega_0^2\tau_c^2} + \frac{2\tau_c}{1+4\omega_0^2\tau_c^2}\right) \quad (3)$$

for spin-spin relaxation[13, 14]. Here, γ_I and γ_S are the gyromagnetic ratio of the interacting nuclei, $\hbar$ is Planck's constant divided by 2π, r is the distance between interacting spins and ω_o is the resonance frequency of the system. For a sample of water at room temperature in a magnet operating at 300MHz, T_1 is approximately equal to T_2 because the correlation time of the molecular field fluctuations due to rotational molecular motion τ_c is much shorter (on the order of 10^{-13} s) than $1/\omega_o$ (on the order of 10^{-9} s). This system is known as being in the motional averaging regime $1/\omega_o >> \tau_c$ because the rapid motion of the molecules quickly averages out the magnetic field interactions. As the experimental frequency ω_o increases or the correlation time τ_c of the magnetic field fluctuations increases, the dependence of T_2 on the zero-frequency term increases, and the two relaxation times T_1 and T_2 diverge when $1/\omega_o = \tau_c$. For fixed correlation time, T_1 and T_2 decrease with increasing frequency until $1/\omega_o = \tau_c$, then T_1 increases and T_2 decreases. Long correlation times, as is the case in highly viscous or solid materials thus generate long T_1 and short T_2. Translational diffusion through magnetic field susceptibility gradients during the echo time 2τ impacts T_2 and increases with applied field strength and decreases with decreasing diffusion coefficient.

EXPERIMENTAL

NMR measurements were performed on a 300 MHz Bruker magnet using a 5 mm radio frequency (rf) coil networked to an AVANCE III spectrometer. Crushed oil shale samples were placed in a 5 mm NMR test tube and filled to a height of approximately 2 inches, which completely fills the active measurement volume of the probe. The rf pulse durations were 4.5 μs for the 90 degree pulse and 9 μs for the 180 degree pulse. A sweep width of 1 MHz was used for signal digitization. Spin-spin T_2 relaxation distributions were measured using a standard CPMG sequence acquiring 6000 echoes with τ = 11 μs giving an echo time of 22 μs. Spin-lattice spin-spin correlation T_1-T_2 data were acquired using the same rf pulse durations and echo times with an inversion recovery sequence encoding for T_1 followed by the CPMG acquisition sequence for T_2. Inversion recovery times were spaced logarithmically in 32 increments between $1x10^{-5}$ to 100 s. The 2D correlation data were analyzed using a 2D inverse Laplace transform algorithm[15, 16]. Using these experimental parameters and analysis on a blank sample results in relaxation time peaks less that 1% of the data peaks indicating the impact of noise and rf timing parameters is negligible. The oil shales measured to date in this study represent a range of materials from regions around the world. These include Ordovician Narva-E kukersite (Estonia); Eocene Green River Formation Mahogany zone and Garden Gulch member (Colorado, USA); Permian Irati Formation marinite (Brazil); Permian Glen Davis and Temi torbanites, Cretaceous Julia Creek marinite, Rundle and Stuart lamosites (Australia); Carboniferous Pumpherston torbanite (Scotland); Cretaceous Ghareb marinite (Israel and Jordan); Permian Phosphoria Formation shale (Montana, USA); Mississippian-Devonian New Albany marinite (Indiana, USA); Cretaceous Timahdit marinite (Morocco); and Cambrian Alum marinite (Sweden).

RESULTS

A subset of the T_2 and T_1-T_2 results are shown in Figures 1-4. For all samples tested, the T_2 time distribution ranges between 10 μs and 10 ms, with most of the signal concentrated at the shortest relaxation times. The kerogen within the shale matrix will primarily have a very short T_2 time if

it is in a glassy polymer state. The T_1-T_2 correlation results for all samples showed the same range of T_2 times as the one dimensional CPMG measurement as expected, but the distribution of relaxation times is divided into two different primary T_1 times. This separation in the T_1 direction may come from the different molecular species within the kerogen having different correlation times of molecular motion due to molecular size or structure. A long T_1 time (over ~ 10 s) and short T_2 (~ 10 μs) is associated with solid like species with very restricted motion and thus long correlation time for intramolecular dipolar coupling. All samples tested had similar trends in the T_1 component distribution but with significant differences in the exact values of T_1 and the relative weight of the distributions at each value. Figure 1 shows the results for Kukersite, which exhibits the long T_1 (over ~ 10 s) and a T_1 component (~500 ms) at the short T_2 (~ 10 μs). In Figures 2 and 4, the Green River and New Albany samples both have a short T_1 component of ~50 ms at the short T_2 (~ 10 μs), while in Figure 3 the Julia Creek sample has T_1 components below ~1 ms. One interpretation of this is that for liquids in the motional averaging regime $T_1 \sim T_2$, so the indication is that the Julia Creek oil shale has a kerogen population which is molecularly more mobile due to the molecular structure of the kerogen but is in a restricted environment which generates the short relaxation times. The full interpretation of these data is beyond the scope of the discussion here and is ongoing.

CONCLUSIONS

Application of high field NMR measurements which have been broadly applied to conventional porous media composed of a fluid filled solid matrix provide differentiation between oil shales. Significant research effort is required to further interpret the data in the context of existing models of kerogen molecular composition and crosslink network structure and the distribution and interaction of the kerogen with the mineral matrix. Data such as this can help inform similar low field NMR data on shales and increase fundamental understanding of oil shale chemical and physical structure.

ACKNOWLEDGEMENTS

JDS and SLC thank the NSF MRI Program and the M.J. Murdock Charitable Trust for equipment funding. Any use of trade, product or firm names is for descriptive purposes only and does not imply endorsement by the U.S. Government.

REFERENCES

1. Palmer, A.R. and G.E. Maciel, *Relaxation Behavior in the Carbon-13 Nuclear Magnetic Resonance Spectrometric Analysis of Kerogen with Cross Polarization and Magic-Angle Spinning.* Analytical Chemistry, 1982. **54**: p. 2194-2198.
2. Mao, J., et al., *Chemical and nanometer scale structure of kerogen and its change during thermal maturationinvestigated by advanced solid state 13C NMR spectroscopy.* Geochimica Et Cosmochimica Acta, 2010. **74**: p. 2110-2127.
3. Cao, X., J. Yang, and J. Mao, *Characterization of kerogen using solid-state nuclear magnetic resonance spectroscopy: A review.* International Journal of Coal Geology, 2013. **108**: p. 83-90.

4. Parks, T.J., et al., *Molecular Properties and Thermal Transformations of Oil Shale Kerogens from in Situ 1H NMR Data.* Energy & Fuels, 1988. **2**: p. 185-190.
5. Kleinberg, R.L. and J.A. Jackson, *An Introduction to the History of NMR Well Logging.* Concepts in Magnetic Resonance, 2001. **13**(6): p. 340-342.
6. Song, Y.-Q., et al., *Magnetic resonance in porous media: Recent progress.* Journal of Chemcial Physics, 2008. **128**(052212).
7. Brownstein, K.R. and C.E. Tarr, *Importance of classical diffusion in NMR studies of water in biological cells.* Physical Review A, 1979. **19**(6): p. 2446-2453.
8. Song, Y.-Q., Venkataramanan, L., Hurlimann, M.D., Flaum, M., Frulla, P., Straley, C., *T1-T2 Correlation Spectra Obtained Using a Fast Two-Dimensional Laplace Inversion.* Journal of Magnetic Resonance, 2002. **154**: p. 261-268.
9. Hurlimann, M., L. Burcaw, and Y.-Q. Song, *Quantitative characterization of food products by two-dimensional D-T-2 and T-1-T-2 distribution functions in a static gradient.* Journal of Colloid and Interface Science, 2006. **297**(1): p. 303.
10. Washburn, K.E. and J.E. Birdwell, *Updated methodology for nuclear magnetic resonance characterization of shales.* Journal of Magnetic Resonance, 2013. **in press**.
11. Zeszotarski, J.C., et al., *Imaging and mechanical property measurments of kerogen via nanoindentation.* Geochimica Et Cosmochimica Acta, 2004. **68**(20): p. 4113-4119.
12. Carr, H.Y. and E.M. Purcell, *Effects of Diffusion on Free Precession in Nuclear Magnetic Resonance Experiments.* Physical Review, 1954. **94**(3): p. 630-638.
13. Kleinberg, R.L., Kenyon, W.E., Mitra, P.P., *Mechanism of NMR Relaxation of Fluids in Rock.* Journal of Magnetic Resonance Series A, 1994. **108**: p. 206-214.
14. Blümich, B., *NMR Imaging of Materials*2000, Oxford: Clarendon Press.
15. Venkataramanan, L., Song, Yi-Qiao, Hurlimann, Martin D., *Solving Fredholm Integrals of the First Kind With Tensor Product Structure in 2 and 2.5 Dimensions.* IEEE Transactions on Signal Processing, 2002. **50**(5): p. 1017-1026.
16. Godefroy, S. and P.T. Callaghan, *2D relaxation/diffusion correlations in porous media.* Magnetic Resonance Imaging, 2003. **21**(3-4): p. 381-383.

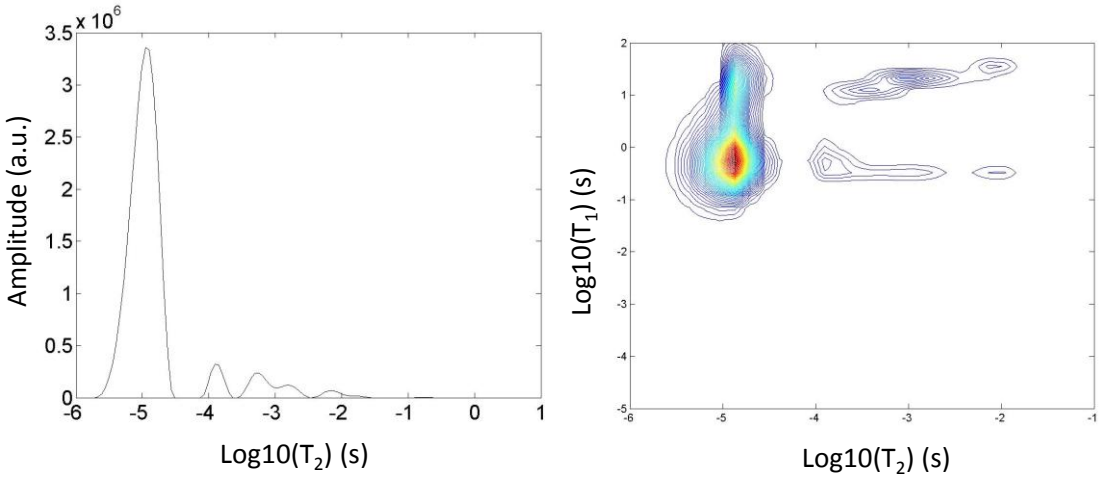

Figure 1. T_2 distribution and T_1-T_2 correlation for Kukersite

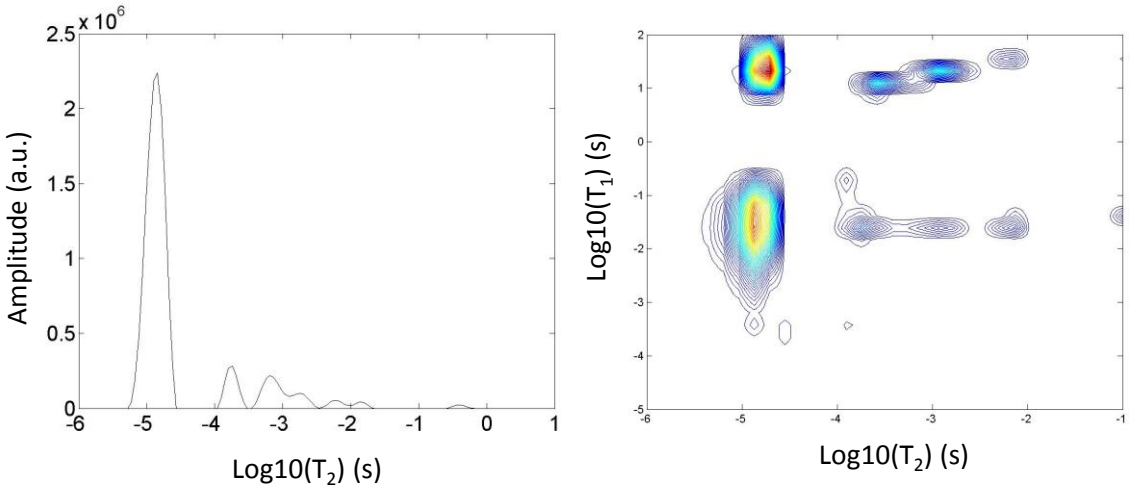

Figure 2. T_2 distribution and T_1-T_2 correlation for Green River

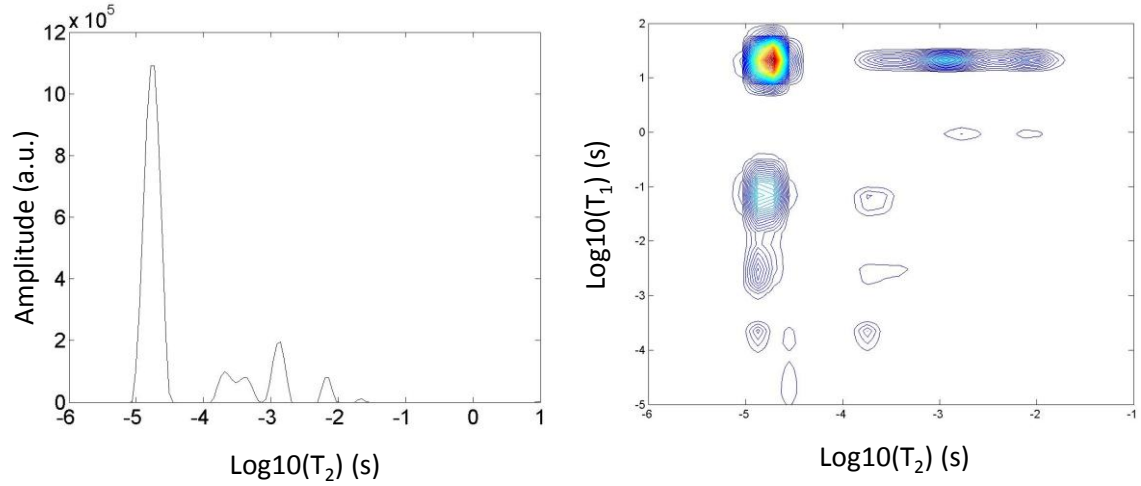

Figure 3. T_2 distribution and T_1-T_2 correlation for Julia Creek.

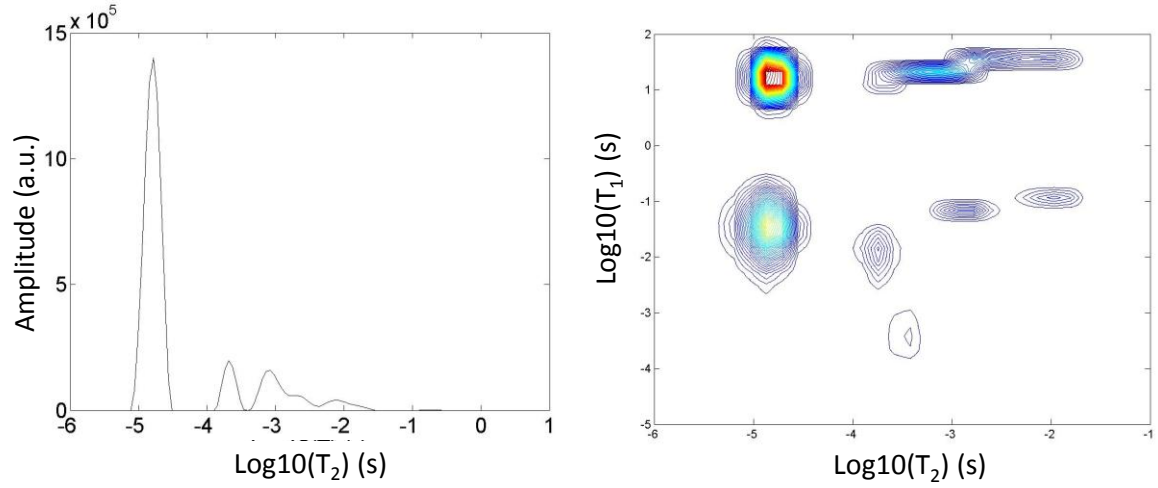

Figure 4. T_2 distribution and T_1-T_2 correlation for New Albany.